Mohammed Boura[1], Ali Benzegaou[2], Brahim Mebarki[3], Mohammed Hadj Meliani[4], Bassam G.N. Muthanna[4,5]*

A MECHANICAL PERFORMANCE STUDY AND SIMULATION OF A HYBRID ELECTRIC VEHICLE POWERED BY Ni-MH BATTERY

ISTRAŽIVANJE MEHANIČKIH PEFORMANSI I SIMULACIJA HIBRIDNOG ELEKTRIČNOG VOZILA SA Ni-MH BATERIJOM

Originalni naučni rad / Original scientific paper
UDK /UDC:

Rad primljen / Paper received: 19.9.2020

Adresa autora / Author's address:
[1)] Department of Technology, TAHRI Mohammed University of Bechar, Bechar, Algeria email: b.mido@yahoo.fr
[2)] Laboratory of Mechanics: L2ME, TAHRI Mohammed University of Bechar, Bechar, Algeria
[3)] ENERGARID Laboratory, TAHRI Mohammed University of Bechar, Bechar, Algeria
[4)] LPTPM, Hassiba Benbouali University of Chlef, Chlef, Algeria email: m.hadjmeliani@univ-chlef.dz
[5)] LRM, Hassiba Benbouali Univ. of Chlef, Chlef, Algeria

Keywords
- hybrid energy source
- DC-DC converters
- battery
- hybrid electric vehicle (HEV)

Ključne reči
- hibridni izvor energije
- DC-DC konvertori
- baterija
- hibridno električno vozilo (HEV)

Abstract

Cars are used in daily life in today's society, but noise pollution, greenhouse gas emissions and increased fuel consumption are constantly increasing. Hybrid electric vehicles are recommended to reduce fossil fuel resources and climate change affecting the planet. Hybrid electric vehicles have a low storage capacity, which is one of the most important parameters for the acceptability of HEV. This article aims to simulate the mechanical performance of a Ni-MH-powered hybrid electric vehicle in Matlab environment. The study focuses on Ni-MH battery controlled by DC-DC converter power supply for HEV. Performance of the proposed strategy controller provides adequate simulation results. The proposed control law increases the autonomy of the HEV utility under several speed variations. In addition, future industrial vehicles must take into account the choice of battery material during design stages. Battery model selection is important, and with the increasing emphasis on vehicle range and performance, Ni-MH battery can provide a viable alternative, as reported in this study.

Izvod

Automobili su danas u svakodnevnoj upotrebi, međutim, zagađenja bukom i emisijom gasova staklene bašte su u stalnom porastu. Preporučuju se hibridna električna vozila (HEV) radi smanjenja upotrebe resursa fosilnih goriva, a i zbog klimatskih promena. Hibridna električna vozila imaju mali kapacitet nosivosti, što je jedan od najvažnijih parametara za prihvatanje HEV. Cilj rada je simulacija mehaničkih performansi hibridnog električnog vozila sa Ni-MH baterijom u okruženju Matlaba. Istraživanja se fokusiraju na izvoru energije tipa Ni-MH baterije sa DC-DC konvertorom za HEV. Performanse predloženog strateškog konvertora su vidljive iz adekvatnih rezultata simulacije. Predloženi konvertor produžava autonomiju sistema HEV u uslovima nekoliko varijacija brzine. Pored toga, kod budućih industrijskih vozila je potrebno uzeti u obzir izbor materijala baterije u fazama projektovanja. Izbor tipa baterije je bitan, a sa sve većim izazovima autonomije i performansi vozila, baterija Ni-MH može biti odgovarajuća alternativa, kao što je razmotreno u ovom istraživanju.

INTRODUCTION

Generally, industrial pollution such as CO_2 emissions is considered as a huge disaster that should be eliminated and disposed /1/. In this fact, energy scarcity and environmental pollution have become a serious issue, resulting in the development of new electric vehicles worldwide /2, 3/. Among them, Hybrid Electric Vehicles (HEVs) can significantly reduce consumption and pollutant emissions compared to traditional vehicles, whose potential has been widely studied in recent decades /4/. Therefore, HEV fuel-saving technologies are targeted, such as regenerative braking control /5/ and Energy Management Strategy (EMS), /6/. Problems associated with hydrocarbon-fuelled vehicles, including environmental damage caused by their emissions and sustainability of current hydrocarbon-based transportation infrastructure.

Unfortunately, the hydrocarbon combustion has a major influence on the global environment. It is responsible for 80% of greenhouse gas emissions, which are the main cause of climate warming and air pollution /7/. To overcome these problems, governments and automobile manufacturers must develop a new generation of vehicles based on environmentally friendly energy use technologies /8, 9/. Most of zero emission commercial vehicles (ZEVs) available today are purely electric vehicles (EVs) powered by batteries. Battery technology is one of the most important areas of research regarding reliability and commercial popularity of this alternative mode of transportation, the battery is a very crucial

component of the powertrain /13/. Nickel metal hydride (Ni -MH) batteries have dominated automotive applications since the 1990s due to their overall performance and best available combination of energy and power densities, thermal performance and cycle life. They are maintenance-free, require simple and inexpensive charging and electronic control, and are made of environmentally friendly recyclable materials. NiMH cell capacity is relatively high, but its potential is 1.35 V. Gravimetric energy density is about 95 Wh/kg and volumetric energy is about 350 Wh/L, /11-13/.

Battery must provide sufficient energy, offer high energy efficiency, high current discharge, and good charge acceptance through regenerative braking, high cycle time and calendar life and abuse tolerance capacity. It should also meet the necessary temperature and safety requirements. Chemical batteries consist of lead acid batteries; nickel-based batteries, such as nickel/iron, nickel/cadmium, and nickel-metal hydride (Ni-MH) batteries. The DC-DC converter is used with a control strategy to provide the energy required by HEV and the propulsion system.

Most new HEVs also use regenerative braking, which allows the electric motor to operate as a generator to recover energy that would have been lost through heat dissipation and friction, improving energy efficiency and reducing brake wear. Sim Power Systems (SPS) integrated battery model is used in the complete simulation of a HEV powertrain. In this context, the objectives of this work focus on the mechanical performance study and simulation of a hybrid electric vehicle powered by Ni-MH battery. The paper is organised as follows: The following two sections describe HEVs, while the section afterwards presents the Energy Management System. The results are then discussed, and are finally summarised, and the conclusions are drawn.

HYBRID ELECTRIC VEHICLE DESCRIPTION

Figure 1 shows that the opposition forces acting on the vehicle's movement are: rolling resistance force F_{tire} due to friction of the vehicle's tires on the road; aerodynamic drag force F_{aero} caused by friction on the body moving in the air; and climbing force F_{slope} that depends on the road slope, /14-16/. Rolling resistance force F_{tire} due to friction of the vehicle's tires on the road is defined by:

$$F_{tire} = mgf_r \,, \tag{1}$$

where: m is vehicle total mass; g is gravity acceleration: f_r is the rolling resistance force constant. The aerodynamic drag force F_{aero} caused by friction on body moving in the air is defined as follows:

$$F_{aero} = \frac{1}{2}\rho_{air} A_f C_d V^2 \,, \tag{2}$$

where: ρ_{air} is air density; A_f is the frontal surface area of the vehicle; C_d is aerodynamic drag coefficient; V is the vehicle speed. The climbing force F_{slope} which depends on road slope is defined as:

$$F_{slope} = mg\sin(\beta) \,, \tag{3}$$

where: β is road slope angle, /17-18/. The total resistive force is equal to Fr and is the sum of the resistance forces, defined as:

$$F_r = F_{tire} + F_{aero} + F_{slope} \,. \tag{4}$$

Values for these parameters are shown in Table 1.

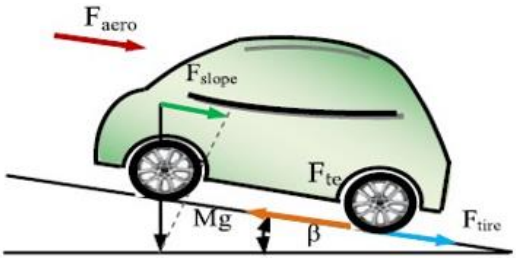

Figure 1. Forces acting on a vehicle moving on slope road.

Table 1. Electric vehicle hybrid model parameters.

R	0.3 m	A_f	2.16 m^2
M	1200 kg	C_d	0.26
f_r	0.01	ρ_{air}	1.2 kg/m^3

HYBRID ELECTRIC VEHICLE MODELS

Traditionally, HEVs are considered to be vehicles that combine features of conventional, i.e. internal combustion engines (ICE), and electric vehicles (i.e. using only batteries). In other words, HEVs combine an electric powertrain with a conventional internal combustion engine powertrain. The proposed performance study introduces hybrid powertrain configurations: in a hybrid parallel electric vehicle (HPEV), the wheels are driven either by ICE or electrical motor or by both of them. Therefore, HEVs can be powered by an ICE and an electric motor in series or in parallel. Thus, braking energy recovery is a significant advantage for both hybrid configurations.

Hybrid parallel electric vehicle modelling

Figure 2 shows that in a parallel configuration, the vehicle wheels are driven either by an ICE and an electrical motor, or by one of them individually. Indeed, ICE and electrical motor are mechanically coupled to the wheel drive shaft by two clutches. This configuration of the electric motor can be used as a generator to charge the battery by regenerative braking or by absorbing power from the ICE when its output power is greater than the load demand via the wheels.

The addition of two propulsion components (i.e. an internal combustion engine and an electric motor/generator) in this hybrid configuration is a major advantage. Moreover, a small ICE and a small electrical motor can be used to drive the vehicle. However, unlike the series configuration, the parallel configuration is more complex in terms of control strategy and coupling mechanisms.

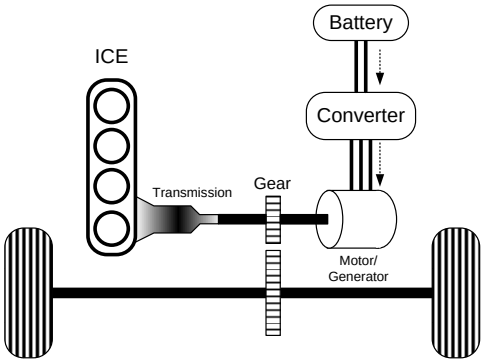

Figure 2. Hybrid electric vehicle with parallel configuration.

Battery model

The battery is considered as the second energy storage system of the HEV using a simple controlled voltage source in series with a constant resistance. This model assumes the same characteristics for charge and discharge cycles. Open voltage source is calculated with a nonlinear equation based on the actual SOC of the battery. The following Eq.(5) provides basic cell reactions of a NiMH battery. The charge reaction is exothermic. The heat produced during the charge process must be released to avoid a continuous temperature rise of the cells, /11-12, 19/.

$$M + Ni(OH)_2 \underset{\text{discharge} \leftarrow}{\overset{\text{charge} \rightarrow}{}} MH + NiOOH \cdot \qquad (5)$$

Figure 3 shows the equivalent circuit of the dynamic model.

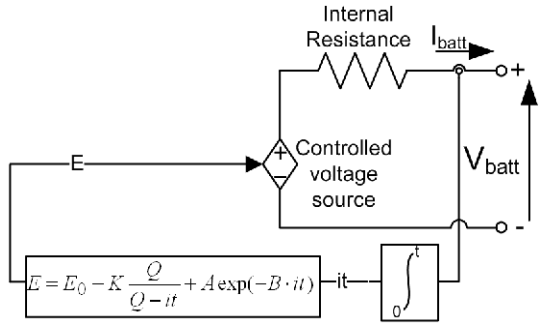

Figure 3. Equivalent circuit of the nickel-metal hydride battery. E - no-load voltage (V); E_0 - battery const. voltage (V); K - polarization voltage (V); Q - battery capacity (Ah); ∫idt -actual battery charge (Ah); A-exponential zone amplitude (V); B - exponential zone time constant inverse $(Ah)^{-1}$; $V_{battery}$ - battery voltage (V); R -internal resistance (Ω); i -battery current (A).

The battery state-of-charge (SOC) is between 0 and 100%. The complete SOC for fully charged battery is 100% and for an empty battery is 0%. The SOC can be defined by Eq.(6):

$$SOC = 100\left(1 - \frac{Q1.05}{\int idt}\right). \qquad (6)$$

Figure 4 explains the different state of discharge curve, the first section represents the exponential voltage drop when battery is charged. Depending on the battery type, this area is more or less wide. The second section represents the charge that can be extracted from the battery until the voltage drops below battery nominal voltage. Finally, the third section represents the total discharge of the battery, when the voltage drops rapidly. NiMH battery parameters used in the proposed propulsion system are illustrated in Table 2.

Table 2. Nickel metal hydride parameters.

Rated capacity	6.5 Ah
Nominal voltage	200 V
Maximum capacity	7 Ah
Nominal discharge current	1.3 A
Exponential voltage	1.28 V
Internal resistance	2 mΩ
Rated capacity	6.5 Ah
Fully charged voltage	1.39 V
Capacity nominal voltage	6.25 Ah
Exponential capacity	1.3 Ah
Exponential voltage	1.28 V

ENERGY MANAGEMENT SYSTEM

The energy management system presented in Fig. 5 uses a simple algorithm based on a threshold logic. This system aims to develop, depending on the position of the vehicle's pedal and speed, the control of the entire powertrain whose role is to choose at every moment the best distribution of power between different energy sources in a manner to minimise fuel consumption and pollutant emissions. Stateflow®, /21/, is used to illustrate different operating modes of the hybrid powertrain and the transition of an energy source to another. Four operating modes are possible: Starting, Acceleration, Cruise and Braking.

The vehicle's start is powered by the electric motor; the idea is to have an all-electric mode and keep the engine off. During a high acceleration demand, the electric motor delivers its maximum power, it is mainly powered by the battery and the generator which is driven by the engine. The engine operates in its optimal performance zone, because when torque demand is high, the engine delivers its maximum power. In cruise mode, the planetary gear distributes the power generated by the internal combustion engine, it drives directly to the wheels and generator, which in turn provides the necessary power to run the electric motor, while assisting in the vehicle traction, too. During the vehicle's braking or deceleration phase, the electric motor operates as a generator and regenerates the kinetic energy of the braking to recharge the battery.

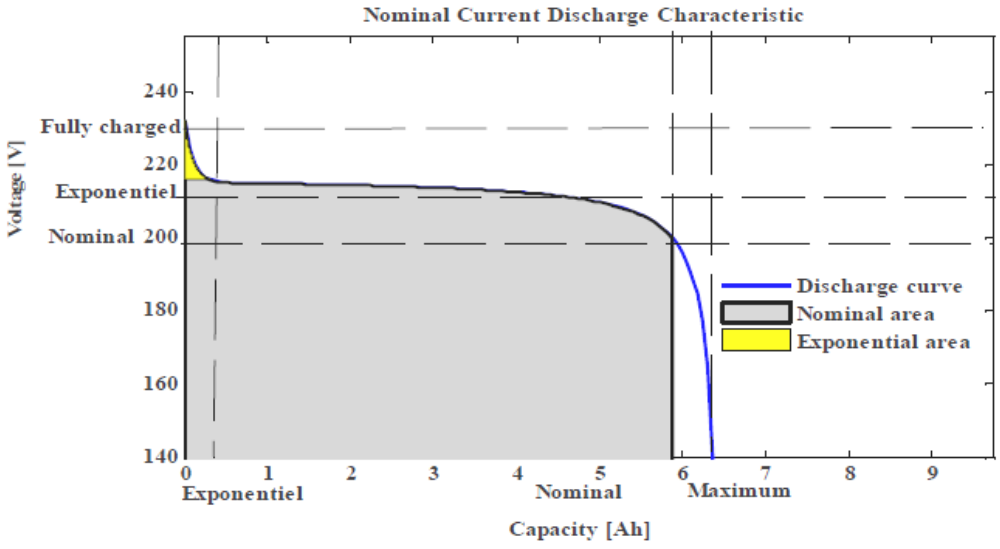

Figure 4. Nickel metal hydride battery typical discharge curve, /20/.

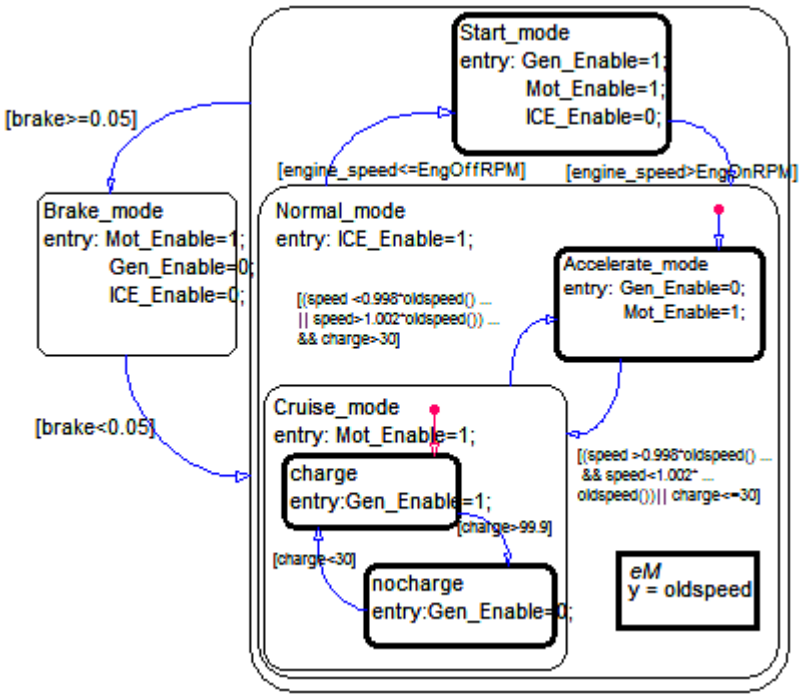

Figure 5. Mode logic modelled with Stateflow®, /21/.

RESULTS AND DISCUSSION

Simulations for normal operation cases consider the Extra Urban Driving Cycle (EUDC) segment that is added after the fourth ECE cycle to include more aggressive and high-speed driving modes, as shown in Fig. 6. Extra-urban cycle is carried out following the urban cycle. It lasts 400 seconds and represents 7 km of travelled distance at an average speed of 62.6 km/h. Like the urban cycle, accelerations remain at a low level. The maximal speed of the EUDC cycle is 120 km/h, which corresponds to the maximal speed allowed on the motorway in many European countries.

This level is maintained for only 10 seconds over the entire cycle during the extra-urban cycle. The driver is allowed to use all gear ratios. The first 3 gears are only used in the acceleration phase until the first landing at 70 km/h. Over the duration of the extra-urban cycle, they are only used for 22 seconds compared to 99 seconds for the fourth gear and 233 seconds for higher gears. Landing at 50 km/h, lasting nearly 70 seconds, is done this time in the 4th gear (unlike the urban cycle where the same level is performed in 3rd gear).

A HPEV model is developed as shown in Fig. 2 to ensure optimal performance through appropriate component sizing and subjective comparison. DC electrical motor and Ni-MH battery are chosen. Simulation tests are conducted while changing the size of both the electrical motor and ICE over a certain power range. However, if the engine size varies from 30 to 80 kW and the current battery capacity varies from 8.1 to 90 Ah (Table 3), the engine size varies from 30 to 80 kW and the vehicle gear ratio varies from 0.7 to 4.1 (Table 4). Table 5 presents technical specifications for this influence factor: mass and drag coefficient. Simulation tests are conducted with EUDC drive cycle and with different combinations of engine, electrical motor, and battery capacities. The performance results in terms of fuel economy, drivability, efficiency, and emissions are presented in Table 5. The best performance is achieved with 120 km/h maximal speed, a battery of 90 Ah with a capacity of 80 kW for the ICE. Full performance results are detailed in Table 3.

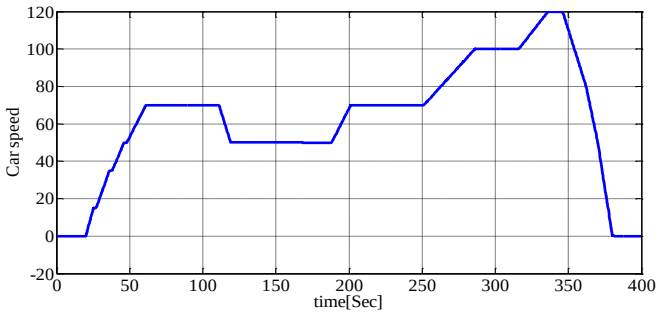

Figure 6. EUDC cycle.

Table 3. Performance simulation results of HEV model with different combinations of engine and battery.

	ICE = 30 kW				ICE = 50 kW				ICE = 70 kW				ICE = 80 kW			
Battery current (Ah)	8.1	30	60	90	8.1	30	60	90	8.1	30	60	90	8.1	30	60	90
Fuel economy gasoline equivalent (L/100 km)	2.859	2.647	2.454	2.278	2.863	2.651	2.458	2.282	2.865	2.653	2.46	2.284	2.866	2.654	2.461	2.285
Maximum speed (km/h)	120	120	120	120	120	120	120	120	120	120	120	120	120	120	120	120
CO_2 emission (g/km)	66.9	62	57.5	53.4	67	62	57.6	53.5	67	62	57.6	53.5	67.1	62.1	57.6	53.5

Table 4. Performance simulation results of HEV model with different combinations of engine and battery.

	ICE = 30 kW				ICE = 50 kW				ICE = 70 kW				ICE = 80 kW			
Vehicle gear ratio	0.7	2.3	3.1	4.1	0.7	2.3	3.1	4.1	0.7	2.3	3.1	4.1	0.7	2.3	3.1	4.1
Fuel economy gasoline equivalent (L/100 km)	2.933	3.137	3.579	4.49	2.932	3.142	3.599	4.93	2.932	3.145	3.608	5.196	2.932	3.145	3.611	5.199
Maximal speed (km/h)	120	120	95	72	120	120	95	72	120	120	95	72	120	120	95	72
CO_2 emission (g/km)	68.7	73.5	83.8	105.1	68.7	73.5	84.3	115.5	68.7	73.7	84.5	121.9	68.7	73.7	84.6	121.8

Table 5. Performance simulation results of HEV model with different combinations of mass and drag coefficient.

	m = 1200 kg				m = 1459 kg				m = 1936 kg				m = 2393 kg			
Drag coefficient	0.6	0.64	0.67	0.7	0.6	0.64	0.67	0.7	0.6	0.64	0.67	0.7	0.6	0.64	0.67	0.7
Fuel economy gasoline equivalent (L/100 km)	3.516	3.573	3.615	3.658	3.642	3.698	3.737	3.767	3.874	3.899	3.892	3.894	3.889	3.884	3.884	3.886
Maximal speed (km/h)	120	120	120	120	120	120	120	120	120	120	120	120	120	120	120	120
CO_2 emission (g/km)	82.34	83.67	84.66	85.67	85.29	86.60	87.52	88.22	90.72	91	91.15	91.19	91	90.96	90.96	91

Performance results in terms of fuel economy and CO_2 emission are listed Table 4. Engine size varies from 30 to 80 kW and the vehicle gear ratio varies from 0.7 to 4.1, as indicated in Table 4.

Aerodynamic drag coefficient is estimated to be higher for the vehicle combinations. To evaluate the impact of a hybrid system configuration for fuel economy, Table 5 presents the technical specifications for this influence factor: mass and drag coefficient.

Influences of various parameters are studied and varied one by one to illustrate the influence on topology, which combines the advantages of hybrid parallel transmission concepts to achieve excellent performance (e.g. fuel consumption, transmission and engine efficiency) for the cases given below. The software tool used to perform all simulations is Matlab-Simulink®, which is widely applied in the industrial environment. Moreover, the various cases studied are simulated for a HEV moving in a straight line.

• *Vehicle Dynamics Subsystem* models all the mechanical parts of the vehicle. The tyre dynamics represent the force applied to the ground, the vehicle dynamics represents the movement influence on the entire system, as shown in Fig. 7.

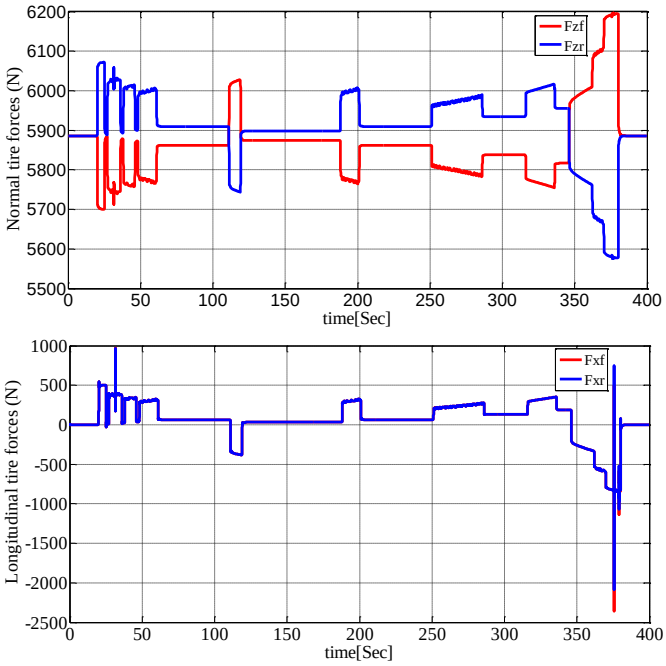

Figure 7. Normal and longitudinal forces.

• *Internal Combustion Engine Subsystem* models the throttle input signal that lies between zero and one and specifies the torque demanded from the engine as a fraction of the maximum possible torque. The vehicle model is used to simulate full throttle acceleration tests to analyse the vehicle performance with each transmission. The vehicle speed traced results for full throttle acceleration, engine speed, engine torque, and engine power test are presented in Fig. 8.

• *Planetary Gear Subsystem* models the power split device. It uses a planetary device which transmits the mechanical motive force from the engine, motor and generator by allocating and combining them. Simulation results of planetary gear sun, carrier and ring are shown in Figs. 9 and 10. Accelerator position signal is shown in Fig. 11. Signal simulation results for vehicle speed are shown in Fig. 12. Figure 13 presents the engine power.

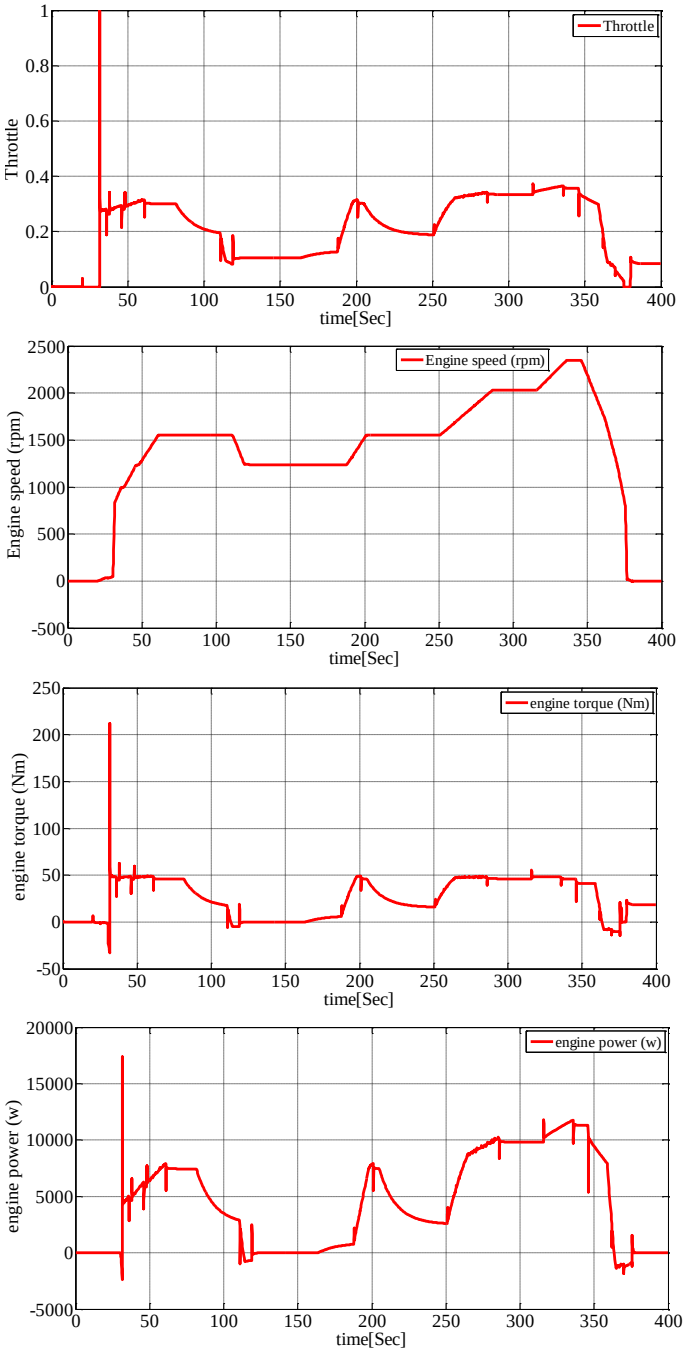

Figure 8. Simulation results of the ICE.

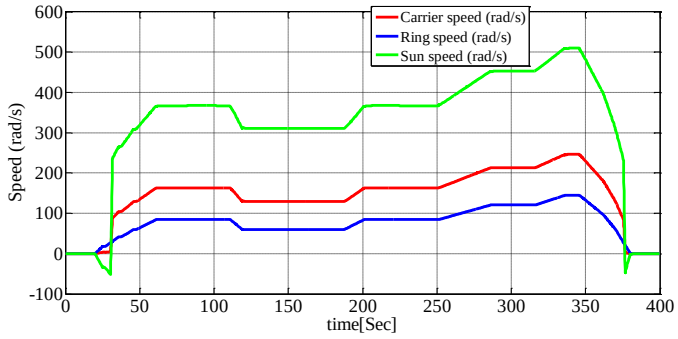

Figure 9. Planetary gear speed.

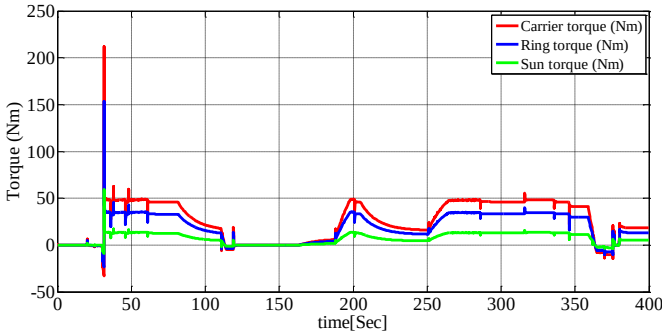

Figure 10. Planetary gear torques.

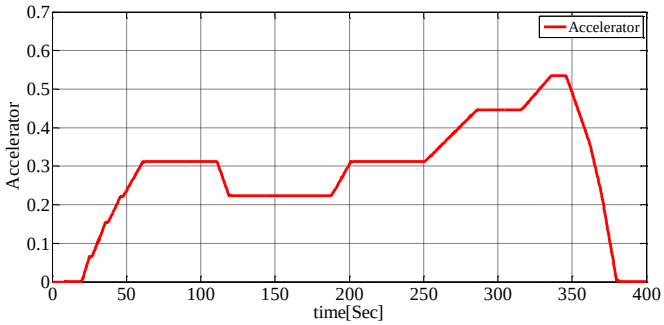

Figure 11. Drive cycle EUDC, acceleration.

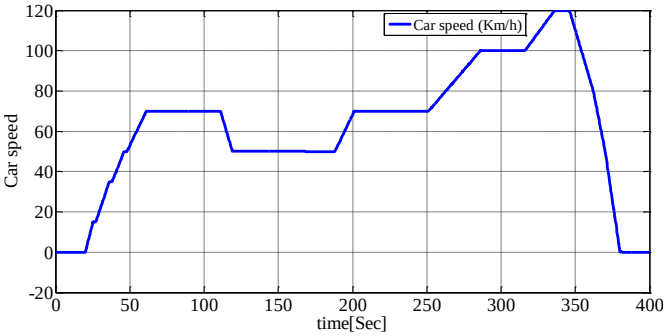

Figure 12. Vehicle speed.

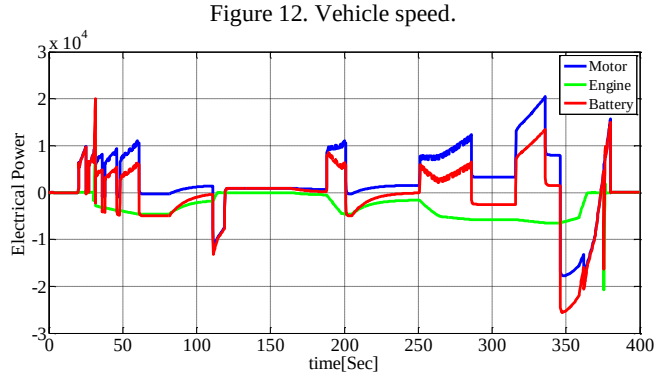

Figure 13. Power.

Different operation modes are shown in Figs. 12 and 13. In low speed driving mode: the vehicle is in pure electric mode, the engine is off, and the traction power is provided by motor as shown in Fig. 13. In boosting mode, at full throttle, the vehicle accelerates, and the engine starts to help the traction power and the motor delivers its maximal power, and is mainly fed by the battery.

In normal driving mode, traction power is provided by both engine and motor, while motor functions as a generator. While in high-speed cruise mode, the engine constantly runs at low speed, where efficiency is high and the planetary gear distributes the power to the wheels and the generator, which in turn provides necessary power to run the motor. During deceleration mode, the engine turns off and the motor functions as a generator recuperating the kinetic energy. Battery capacity is increased and the duration of all electric modes always depends on the state of charge and there is no specific time or range.

The battery state of charge (SOC %) is shown in Fig. 14. The operating range is between 100 and 93 %. The downward trend of the curve reflects the nature of discharge during the short period of simulation. Fluctuating SOC is caused by the battery being fed by regenerative braking.

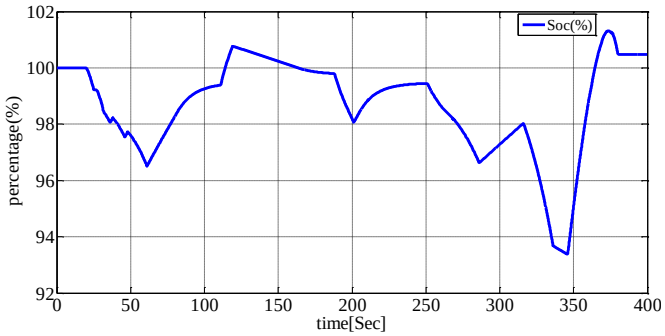

Figure 14. Battery state of charge (SOC).

DC bus voltage of the electrical system is regulated at 500 V, as shown in Fig. 15, thus having a lower current and therefore less loss for the same required power. Bus voltage increases/decreases during periods of acceleration and regenerative braking. Input/output battery voltage in Fig. 16 is maintained around 220 V during acceleration phases. The voltage drops below 220 V to power the engine and during deceleration, the battery recharges by recovering the braking energy.

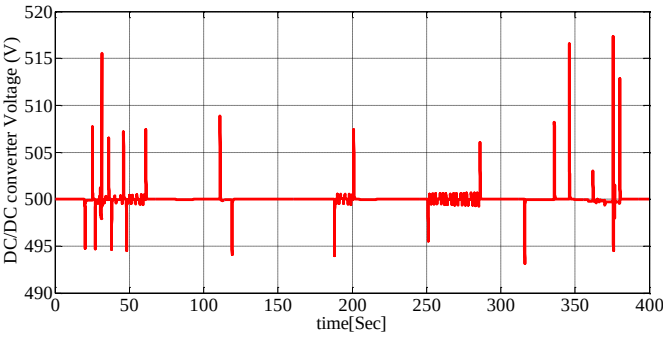

Figure 15. DC/DC converter voltage.

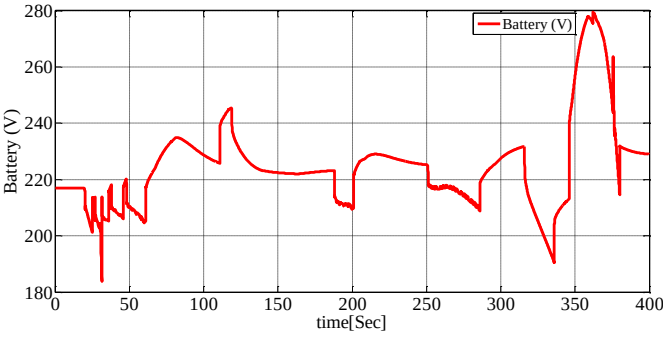

Figure 16. Battery voltage.

CONCLUSION

According to the numerical analysis of this investigation, the obtained results show that the hybrid vehicle is one of the alternatives considered to replace the conventional vehicle, with a performance approximately twice as high as that of a gasoline engine over an urban cycle. Numerical models are carried out using Matlab/Simulink®, which includes vehicle longitudinal dynamics model, ICE model, a speed coupling device model (planetary gear mechanism), vehicle speed, electric motor power, engine torque, and battery power, that are satisfactory, consistent and in accordance with theory showing very good stability over the entire cycle. Ni-MH battery has been demonstrated to have good performance and dynamic characteristics for the electric vehicle propulsion system.

ACKNOWLEDGEMENTS

The authors would like to thank Professor A. BENZEGAOU College for valuable discussion and helpful suggestions during the course of this work.

REFERENCES

1. Amara, M., Bouledroua, O., Hadj Meliani, M., et al. (2018), *Assessment of pipe for CO_2 transportation using a constraint modified CTOD failure assessment diagram*, Struct. Integ. and Life, 18(2): 149-153.
2. Fekaouni, M.F., Maspeyrot, P., Hadj Meliani, M., Youcefi, A. (2019), *Passive structural control of a model car drag by transverse separating plates*. Struct. Integ. and Life, 19(1): 37-44.
3. Li, L., Wang, X., Song, J. (2017), *Fuel consumption optimization for smart hybrid electric vehicle during a car-following process*, Mech. Syst. Signal Process. 87: 17-29. doi: 10.1016/j.ymssp.2016.03.002
4. Xiong, R., Cao, J., Yu, Q. (2018), *Reinforcement learning-based real-time power management for hybrid energy storage system in the plug-in hybrid electric vehicle*, Appl. Energy, 211: 538-548. doi: 10.1016/j.apenergy.2017.11.072
5. Li, L., You, S., Yang, C. (2016), *Multi-objective stochastic MPC-based system control architecture for plug-in hybrid electric buses*, IEEE Trans. Indust. Elec. 63(8): 4752-4763. doi: 10.1109/TIE.2016.2547359
6. Zhang, J., Lv, C., Gou, J., Kong. D. (2012), *Cooperative control of regenerative braking and hydraulic braking of an electrified passenger car*, Proc. Inst. Mech. Eng., Part D: J Autom. Eng. 226(10): 1289-1302. doi: 10.1177/0954407012441884
7. Martinez, C.M., Hu, X., Cao, D., et al. (2017), *Energy management in plug-in hybrid electric vehicles: Recent progress and a connected vehicles perspective*, IEEE Trans. Vehic. Technol. 66(6): 4534-4549. doi: 10.1109/TVT.2016.2582721
8. Barreras, F., Maza, M., Lozano, A., et al. (2012), *Design and development of a multipurpose utility AWD electric vehicle with a hybrid powertrain based on PEM fuel cells and batteries*, Int. J Hydr. Energy, 37(20): 15367-15379. doi: 10.1016/j.ijhydene.2012.06.091
9. Van den Hoed, R. (2007), *Sources of radical technological innovation: the emergence of fuel cell technology in the automotive industry*, J Cleaner Prod. 15(11-12): 1014-1021. doi: 10.1016/j.jclepro.2006.05.032
10. Tang, Y., Yuan, W., Pan, M., Wan, Z. (2011), *Experimental investigation on the dynamic performance of a hybrid PEM fuel cell/battery system for lightweight electric vehicle application*, Appl. Energy, 88(1): 68-76. doi: 10.1016/j.apenergy.2010.07.033
11. Salman, M., Chang, M.F., Chen, J.S. (2005), *Predictive energy management strategies for hybrid vehicles*, In 2005 IEEE Vehicle Power Propul. Conf.: 21-25. doi: 10.1109/VPPC.2005.1554526
12. Larminie, J., Lowry, J., Electric Vehicle Technology Explained, John Wiley & Sons, Ltd., 2003. doi: 10.1002/0470090707
13. Nelson, R.F. (2000), *Power requirements for batteries in hybrid electric vehicles*, J Power Sources, 91(1): 2-26. doi: 10.1016/S0378-7753(00)00483-3
14. Abd El Monem, A.A., Azmy, A.M., Mahmoud, S.A. (2012), *Dynamic modelling of proton exchange membrane fuel cells for electric vehicle applications*, Eng. Res. J. 35(3): 205-214.
15. del Real, A.J., Arce, A., Bordons, C. (2007), *Development and experimental validation of a PEM fuel cell dynamic model*, J Power Sources, 173(1): 310-324. doi: 10.1016/j.jpowsour.2007.04.066
16. Fărcaș, A.C., Dobra, P. (2014), *Adaptive control of membrane conductivity of PEM fuel cell*, Procedia Technol. 12: 42-49. doi: 10.1016/j.protcy.2013.12.454
17. Gasbaoui, B., Chaker, A., Laoufi, A., et al. (2011), *The efficiency of direct torque control for electric vehicle behavior improvement*, Serb. J Elec. Eng. 8(2): 127-146. doi: 10.2298/SJEE1102127G
18. Nasri, A., Gasbaoui, B. (2011), *A novel electric vehicle drive studies based on space vector modulation technique and direct torque control strategy*, J Asian Elec. Veh. 9(2): 1529-1535. doi: 10.4130/jaev.9.1529
19. Gasbaoui, B., Abdelkader, C., Laoufi, A., Alloua, B. (2010), *Adaptive fuzzy PI of double wheeled electric vehicle drive controlled by direct torque control*, Leonardo Electron. J Pract. Technol. 17: 27-46.
20. Ramadass, P, Haran, B., White, R., et al. (2002), *Capacity fade of Sony 18650 cells cycled at elevated temperatures: Part II. Capacity fade analysis*, J Power Sources, 112: 614-620. doi: 10.1016/S0378-7753(02)00473-1
21. Mahapatra, S., Egel, T., Hassan, R., et al. (2008), *Model-based design for hybrid electric vehicle systems*, (No. 2008-01-0085), SAE Tech. Paper. doi: 10.4271/2008-01-0085